Iranian Journal of Materials Science and Engineering, Vol. 20, Number 2, June 2023
RESEARCH PAPER

Effect of Chemical Composition on Microstructure and Hydrophobic Properties of SiO_2-TiO_2@PDMS Coating

Amirreza Sazvar*, Seyed Mohammad Saeed Alavi, Hossein Sarpoolaky

* *amir_sazvar@yahoo.com*

School of Metallurgy and Materials Engineering, Iran University of Science and Technology (IUST), Tehran, Iran

Received: January 2023 **Revised: May 2023** **Accepted: May 2023**
DOI: 10.22068/ijmse.3114

Abstract: *We report a simple and practical approach for the easy production of superhydrophobic coatings based on TiO_2-SiO_2@PDMS. In this study, we used tetraethylorthosilicate (TEOS) and titanium tetraisopropoxide (TTIP) as precursors for the sol-gel synthesis of SiO_2 and TiO_2 particles respectively. Afterward, the surface of nanoparticles was modified by 1, 1, 1, 3, 3, 3-hexamethyldisilazane (HMDS) before being combined with polydimethylsiloxane (PDMS). The hydrophobic property of coatings was evaluated by static contact angle measurements. The phase composition and structural evolution of the coatings were examined by X-ray diffraction (XRD), and Fourier transform infrared spectroscopy (FTIR) analysis. It was shown that changing the weight ratio of the solution composition of the coating can affect the hydrophobicity of the surface. The best sample showed a superhydrophobic property with a 153˚ contact angle which contained (75%TiO_2-25%SiO_2) and PDMS at a weight ratio of 1:1. Moreover, the results showed that the superhydrophobic coating retained its hydrophobic properties up to 450˚C, and at higher temperatures, a super hydrophilic behaviour was observed with a water contact angle close to 0˚. The SiO_2-TiO_2@PDMS coating degraded methylene blue by about 55% and was shown to be capable of photocatalytically decomposing organic pollutants.*

Keywords: *Superhydrophobic coating, Photocatalytic, Sol-gel, Silica, Titania.*

1. INTRODUCTION

The super-hydrophobicity phenomena were initially identified on lotus leaves. Surfaces having a water contact angle (WCA) of more than 150° and a sliding angle of less than 10 are referred to as superhydrophobic [1-3]. Superhydrophobic coatings are widely employed in everyday life and industry, because they may offer substantial liquid repellency and enable self-cleaning [4], anti-icing [5], corrosion resistance [6], oil-water separation [7], and water manipulation [8]. However, due to low transparency, poor durability, difficult preparation procedures, substrate dependency, and high fabrication costs, artificial superhydrophobic coatings are currently limited in their use on a broad scale. Furthermore, new creative non-toxic, and multifunctional materials are required to create flexible superhydrophobic surfaces that match the needs of industrial applications [9].

Dip-coating, liquid flame spray, layer-by-layer assembly, reactive laser etching, and their combinations have all been used to create hydrophobic coatings with super-hydrophobicity and high transparency properties [10].

The textured surface is a frequent feature of several production processes. This texture is necessary for the creation of air pockets (the Cassie-Baxter state) between the surface and droplets, which allows liquids to slide easily. The materials exploited in superhydrophobic coatings should have low surface energy, with the exception of particular textures with re-entrant geometry [11].

Hybrid organic-inorganic composite coatings are very popularly used in fabricating superhydrophobic surfaces since they combine the advantages of both organic and inorganic materials. Inorganic particles are often used to create and adjust nano- or microscale structure on polymer coatings to fabricate composite superhydrophobic coatings [12]. Because of its controlled structure, ideal stability, and low toxicity, various researchers have used silica or titania to develop superhydrophobic surfaces. polydimethylsiloxane (PDMS) resin is frequently used for its high mechanical stability, low surface energy, and superhydrophobic properties [13]. Parkin et al. [14] reported a superhydrophobic photocatalytic coating that incorporated PDMS polymer and functionalized titania nanoparticles by aerosol-assisted chemical vapor deposition (AACVD). Deng et al. [15] have prepared a superhydrophobic coating based on TiO_2–SiO_2@PDMS with good thermal stability and

[Downloaded from cehsat.iust.ac.ir on 2026-09-14]
[DOI: 10.22068/ijmse.3114]

photocatalytic properties. Yang et al. [16] fabricated a coating with a contact angle of 155°. Crupi et al. [17] have investigated the optimal amount of TiO_2 in the TiO_2/SiO_2/PDMS nanocomposite coating. Peng et al. [12] fabricated a photocatalytically stable superhydrophobic and translucent coatings generated from PDMS-grafted-SiO_2/TiO_2@PDMS.

With the use of non-fluorinated materials, in this study, we provide a straightforward technique for fabricating thermally stable and photocatalytic TiO_2–SiO_2@PDMS hybrid films. In this research, the effect of different amounts of titania, silica, HMDS and also PDMS in composition was investigated to find the optimum composition with the highest WCA. To the best of the authors' knowledge, this is the first time the effect of compositions' change is presented. This method for creating multi-functional superhydrophobic surfaces, as well as their potential commercial application in different applications, might provide a simple and low-cost platform for the production and broad uses of the adaptable composite powder.

2. EXPERIMENTAL PROCEDURES

2.1. Materials and Methods

Materials used such as 1,1,1,3,3,3-hexa methyldisilazane (HMDS), tetraethylorthosilicate (TEOS, 98%), titanium isopropoxide (TTIP), ammonia solution (25%), acetic acid (98%), ethanol (90%) were prepared from MERCK company. Sylgard-184 (Silicon Elastomer) (PDMS) was purchased from DOW CORNING. Before usage, the glass substrate was additionally wiped with acid and water.

Silica sol (SiO_2) was obtained by hydrolysis of (TEOS) in the presence of acetic acid and ethanol. The compound used was prepared with the molar ratio [TEOS]: [EtOH]: [CH_3COOH]: [H_2O]= 1: 10:0.5:6. First, half of the ethanol was mixed with TEOS and acetic acid for one day at room temperature. Then the other half of ethanol and water was added dropwise to the above solution for 20 minutes. The pH of the resulting solution was adjusted to about 2 by adding enough 37% hydrochloric acid solution.

Titanium sol was prepared using (TTIP) as a precursor. TTIP was mixed with ethanol and acetic acid for 2 hours with stirring. The compound used was prepared with a volume ratio of [TTIP]: [CH_3COOH]: [EtOH]= 1:2:2. Then the pH of Titania was adjusted to about 2 by adding 37% hydrochloric acid solution. Afterward, solutions of silica and titania sol were converted to gel by adding 25% ammonia solution and adjusting the pH to about 9 and kept overnight to age.

To prepare the hydrophobic SiO_2-TiO_2 gels, 1.67 g of HMDS was mixed with 13.36 g of ethanol and added to 1 g of the hybrid gel mixture, and the resulting mixture was mixed for 20 h at 70°C in a closed container. The resulting hybrid gels were then washed three times with ethanol to remove free HMDSs and then dried at 80°C for 1 h. Hybrid gels used were prepared with three different weight ratios of 75%, 50% and 25% SiO_2 and then modified with HMDS.

0.2 g of HMDS-modified SiO_2-TiO_2 hybrid gel were dispersed in 4 ml of chloroform ($CHCl_3$) for 10 minutes in an ultrasonic bath. Then, 0.2 g of HMDS and 0.15 g of PDMS (Sylgard 184 base elastomer) were added to the above solution and placed in an ultrasonic bath for another 1 hour. 0.01 g of curing agent dissolved in 4 ml of chloroform was added to the above mixture and stirred rapidly for 10 minutes. Also, two other solutions, the first with a ratio of twice the amount of hybrid gel (0.4 g) and the second with a ratio of twice the PDMS (0.3 g) were prepared in the same way. The solution TiO_2-SiO_2@PDMS/$CHCl_3$ was sprayed onto the sliding glass slide and then the glass slide was cured for 1 h at 100°C.

2.2. Characterization

X-ray diffraction (XRD, Bruker) using Cu-K_α radiation was used to study the phase evolution of the synthesized samples. For this experiment, the prepared gel was mixed with 50% titania and 50% silica and heated for 2 h at 450°C. Titania gel was also placed separately in the mentioned conditions. The microstructure and the morphology of the organic-inorganic polymer hybrid on the substrate were examined by scanning electron microscopy secondary electron microscopy (SEM, Zeiss).

The static contact angles (CAs) of a 5 mL water droplet on the surface were measured with a (Pendant Drop Tensiometer, Fars EOR Technologies) at ambient temperature. After covering the glass surfaces and measuring the contact angle, the coating was peeled off and used

[Downloaded from cehsat.iust.ac.ir on 2026-09-14]

[DOI: 10.22068/ijmse.3114]

for Fourier transform infrared spectroscopy (FTIR, Perking-Elmer). The samples were mixed with KBr powder for FTIR measurements from 4000 to 400 cm^{-1} at a resolution of 4 cm^{-1}. For investigation of the photocatalytic properties, the highest CA (Contact Angle) sample solution was added to methylene blue (MB) dilutions, and the mixtures were stirred in the dark for 1 hour. The sample was exposed to UV irradiation for 2 h using a UV lamp.

3. RESULTS AND DISCUSSION

In this study, a nanostructure SiO_2-TiO_2@PDMS superhydrophobic coating was fabricated on a glass substrate by employing the spray technique. The synthesis of silica, titania and their hybridization, particle surface modification, PDMS polymerization, wettability, surface morphology, and photocatalytic properties of the coated sample have been discussed.

To investigate the presence of titania and silica and the hybridization of the mixture of these two substances in the produced sample, a XRD pattern was used and the results have shown in Figure 1. In the XRD pattern of Figure 1 (a), the protrusion in the diagram indicates the presence of an amorphous phase in the sample. It was concluded that the phase of SiO_2 was amorphous SiO_2 because of the existence of a characteristic peak of amorphous material with a nearly symmetrical peak shape and a certain strength at approximately 2θ= 21° [18, 19]. In the hybrid sample, anatase TiO_2 peak at 25.3° is not visible distinctly in XRD pattern, indicating that the crystallinity of TiO_2 loaded on the surfaces of SiO_2 microspheres was low [18] and TiO_2 is highly dispersed in the SiO_2 matrix and the amorphous nature of SiO_2 is prominent in the matrix [20].

The existence of anatase is one of the most crucial requirements for the photocatalytic activity of TiO_2 materials [21]. In order to observe the crystallization of anatase, titania sol was calcined at 450°C, since amorphous silica does not crystallize up to temperatures above 1000°C. Moreover, PDMS decomposes in temperatures more than 450°C [15]. In Figure 1 (b) the main diffraction peaks were indexed to anatase TiO_2 (JCPDS card No. 21-1272, tetragonal structure) [22-24]. Arun Kumar et al. [25] have synthesized TiO_2-SiO_2 nanocomposites by the sol-gel method, and the results of the XRD pattern of their samples are consistent with the results obtained in this article.

It was also suggested that this behavior could be attributed to the low crystallite size of the powder obtained from the sol-gel method [26]. To investigate the Wettability behavior of the coating, the static contact angle of water was measured. To determine the optimal composition of the coating solution, the effect of changing the powder composition and changing the components of the coating solution was investigated. The results are tabulated in Table 1.

The values of water contact angle in TSP1, TSP2 and TSP3 samples are equal to 142°, 146° and 153°, respectively, which indicates the increase of static contact angle of water due to the increasing the percentage of titania in the hybrid composition of gels.

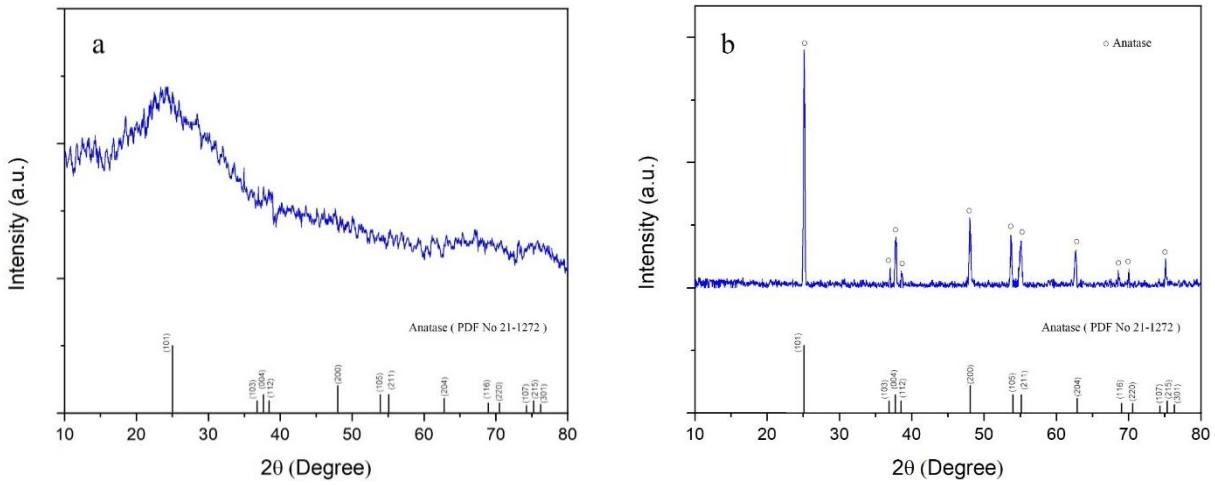

Fig. 1. XRD pattern of the as-synthesized a) TiO_2/SiO_2 nanocomposite, b) TiO_2 nanoparticles

[Downloaded from cehsat.iust.ac.ir on 2026-09-14]

[DOI: 10.22068/ijmse.3114]

Table 1. Characteristics of the prepared coatings

Sample Name	Powder Composition	Amount of Powder (g)	Amount of PDMS (g)	Contact angle (degree)
TSP1	25 %TiO_2– 75% SiO_2	0.2	0.15	142
TSP2	50% TiO_2– 50% SiO_2	0.2	0.15	146
TSP3	75% TiO_2– 25% SiO_2	0.2	0.15	153
TSP4	25 %TiO_2– 75% SiO_2	0.2	0.3	98
TSP5	50% TiO_2– 50% SiO_2	0.2	0.3	127
TSP6	75% TiO_2– 25% SiO_2	0.2	0.3	135
TSP7	25 %TiO_2– 75% SiO_2	0.4	0.15	103
TSP8	50% TiO_2– 50% SiO_2	0.4	0.15	105
TSP9	75% TiO_2– 25% SiO_2	0.4	0.15	112

Increasing the amount of modified powder and PDMS in the coating solution of TSP4 to TSP9 samples reduced the static contact angle of water, while increasing the amount of modified powder had a greater impact on reducing the static contact angle of water.

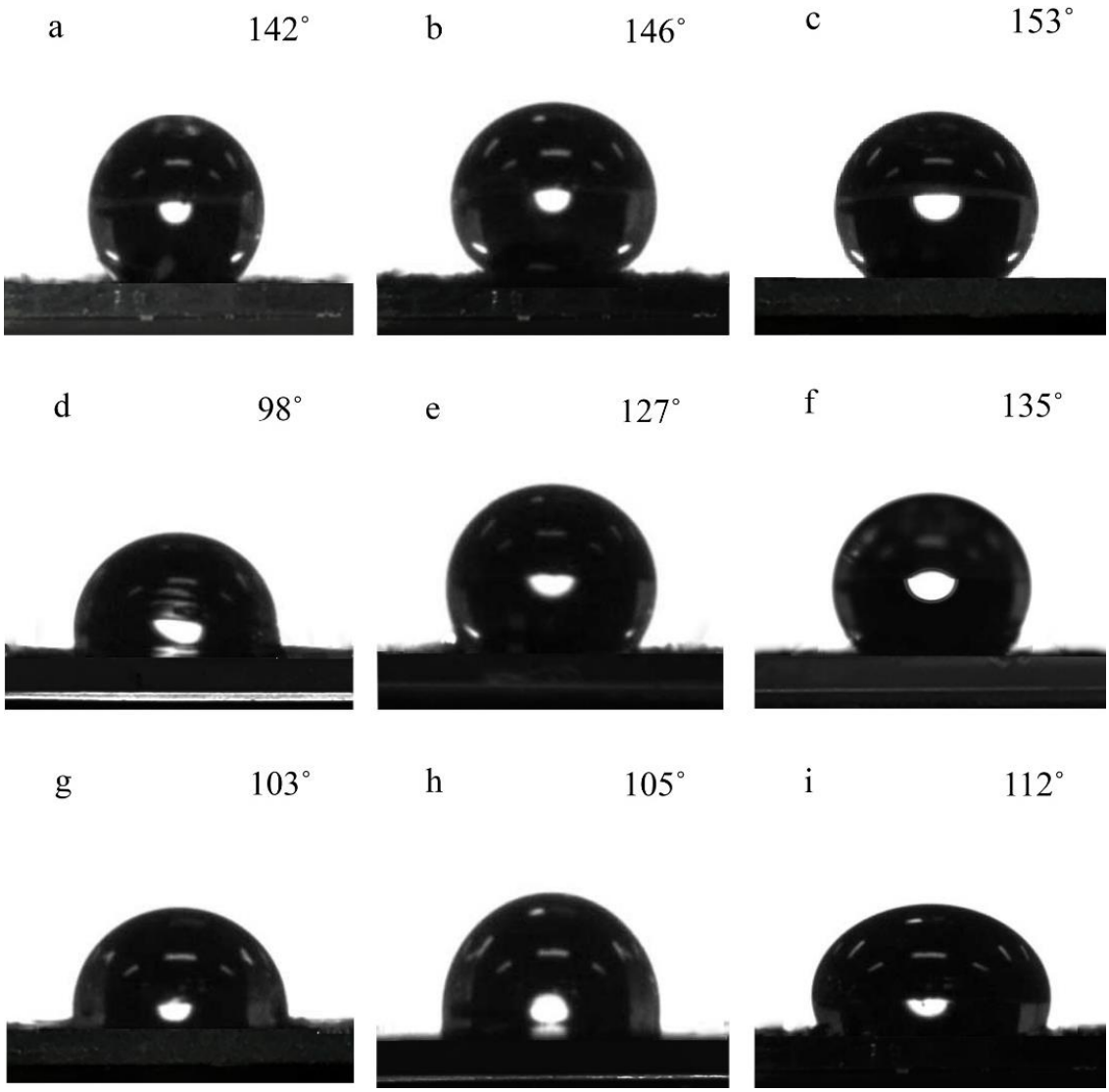

Fig. 2. Image of 5 µL drops of water on the surface of samples a) TSP1, b) TSP2, c) TSP3, d) TSP4, e) TSP5, f) TSP6, g) TSP7, h) TSP8, i) TSP9

[Downloaded from cehsat.iust.ac.ir on 2026-09-14]

[DOI: 10.22068/ijmse.3114]

Modification of particle surface chemistry and creation of micro/nanostructure are the two main factors in creating hydrophobic properties in coatings, and with the presence of these two factors, super-hydrophobic coatings can be made simultaneously. Oxygen-containing functional groups (-OH and -CO_3) increase the surface energy significantly, which strengthens the adhesion between liquid droplets and solid surfaces. Uncoated glass substrate due to the presence of OH-functional groups on the glass surface has a high surface energy that causes water droplets to adhere to the surface and makes the glass surface hydrophilic with a water contact angle of about 30° as shown in Figure 3 (a).

The unmodified nano silica and nano titania powder presents strong hydrophilicity [27, 28]. It is possible by using low surface energy materials and creating surfaces with the desired surface roughness utilizing hierarchical micro/nano-structures to achieve the superhydrophobic feature [29]. Materials employed for chemical modification possess an intrinsically low surface energy due to nonpolar chemistries, and closely packed, stable atomic structures can exhibit water repellency. Examples include polysiloxanes (−Si−O−Si− groups), fluorocarbons (CF_2/CF_3), nonpolar materials (with bulky CH_2/CH_3 groups), or polymers with combined chemistry [30]. Particle surface modification with HMDS, by replacing -CH_3 groups instead of -OH groups, reduces the adhesion force between water molecules and the surface more than the correlation force between the water molecules themselves [26]. This causes a decrease in surface wettability by water droplets, which results in hydrophobicity in the coating made of HMDS-modified particles. Modified particles of different sizes in the range of a few hundred nanometers to a few microns, the static contact angle of water 70° to 120° [15]. More nanometer-modified particles can be placed inside the porosity of the glass substrate than the micron particles, which creates a greater hydrophobic angle. The coating made of HMDS-modified particles has a static water contact angle of about °80 as shown in figure 3 (b).

Coating made of PDMS due to the micro-porous matrix and the presence of -CH_3 functional groups in the structure of PDMS, as shown in part (c) has a static contact angle of water of about 120° which is more than the PDMS coating made by Z.He et al. [31] with a water contact angle of about 107°.

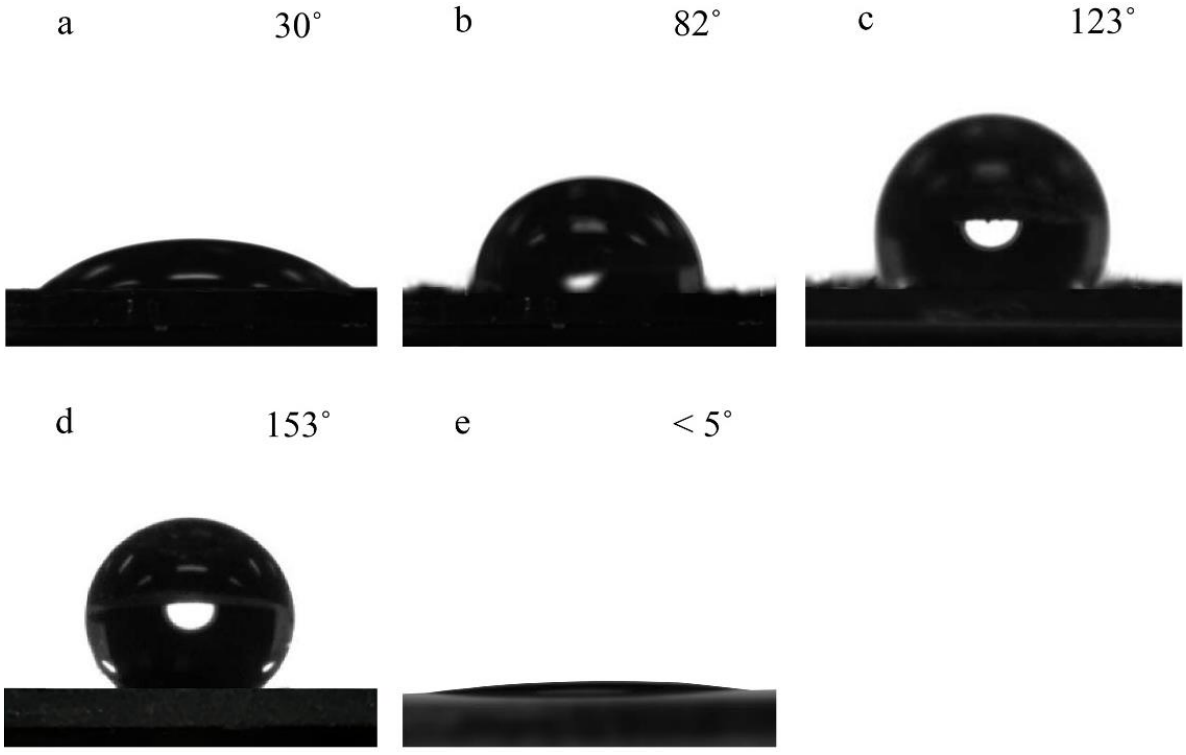

Fig. 3. Image of µL 5 drops of water on the surface of the coating a) Uncoated glass substrate, b) HMDS-modified particle coating, c) PDMS coating, d) TSP3 coating e) TSP3 sample after treating in 450˚ for 2 hours

[Downloaded from cehsat.iust.ac.ir on 2026-09-14]

[DOI: 10.22068/ijmse.3114]

TSP3 coating on a glass substrate which is prepared of PDMS and HMDS-modified nanoparticles due to the creation of porous texture of micro-nano structure, as shown in (d) has a hydrophobic behavior with a static contact angle of water above 150°. The contact angle of a similar coating made by Deng et al. [15] with a water contact angle of about 160° is greater than the TSP3 coating. Moreover, treating the coating with a temperature over 400°C for 2 hours as shown in figure 3 (e) makes the coating super hydrophilic with a contact angle of less than 5°. The cause of the superhydrophilic behavior of the coating is the decomposition of organic groups and the formation of Si–OH and Ti–OH bonds on the surface which is in accordance with other researchers' results [15]. Scanning electron microscopy analysis was performed to examine the coating texture, size and distribution of the modified particles. In figure 4 (a) and at a magnification of 30,000, it can be seen that the hybrid nanoparticles of silica and titania are agglomerated and form particles with dimensions in the range of a few hundred nanometers to a few microns that are scattered inside the porous matrix of PDMS. In (b) and (c) at magnifications 1000x and 250x, the micro-porous texture of the PDMS matrix with a micro-nano structure is shown. The micro-nano structure is due to the dispersion of HMDS-modified particles in the PDMS matrix. Micro-nano structure and air entrapment within micro-porosity are the main causes of superhydrophobicity properties, which can be seen in the TSP3 sample images. Figure 4 (d) presents elemental mapping results of TSP3 sample. Element mapping results shown in Fig. 2 confirmed. The presence of Si, and Ti elements. Also, it should be noted that the intensity of the red color (showing Si element) is higher than yellow (showing Ti element) due to more surface area covered by Si. This approves the lack of anatase phase in the XRD pattern as most of the surface is covered by SiO_2. It is observed in figure 5 (b) that by doubling the amount of PDMS, the porous matrix is no longer formed and the micro-nano structure of the surface is not prepared. On the other hand, a large number of hydrophobic particles are trapped under the PDMS layer and will not affect the hydrophobic behavior of the coating and what affects the hydrophobic behavior is the reduction of surface energy due to $-CH_3$ functional groups in the PDMS matrix.

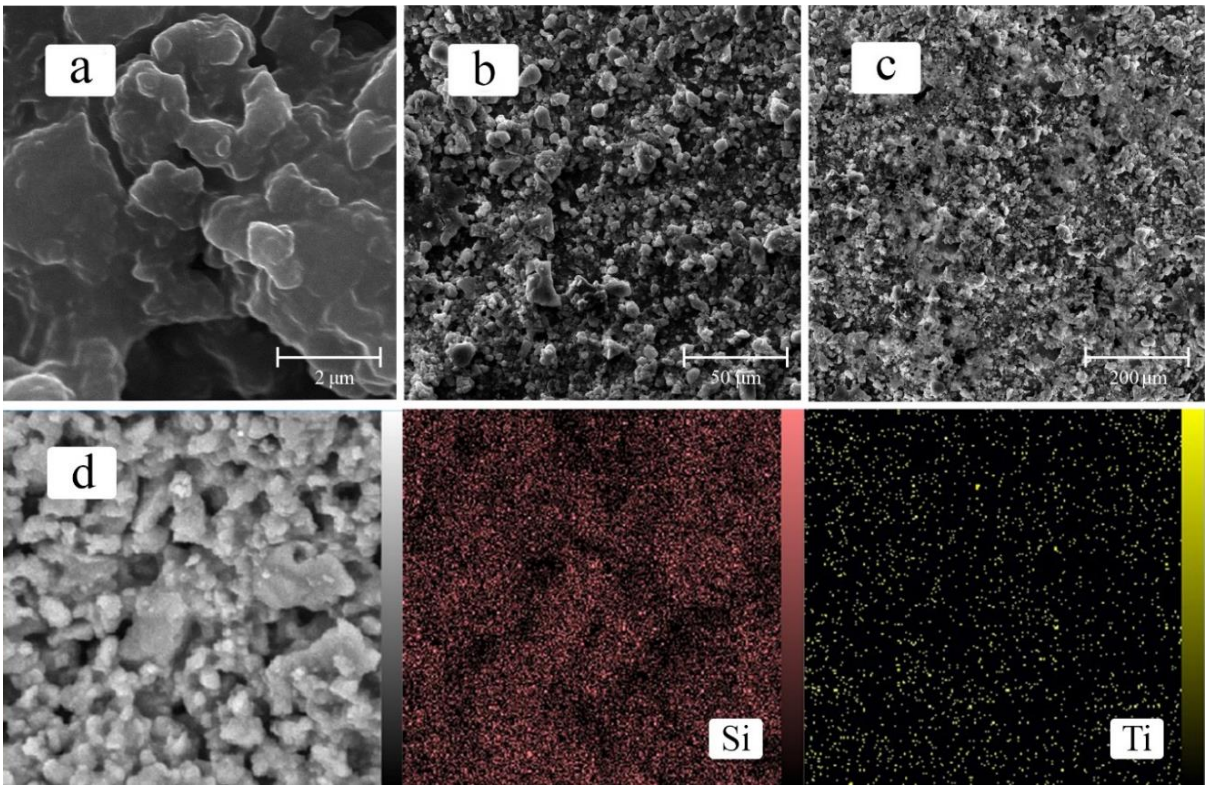

Fig. 4. SEM images of TSP3 with a water contact angle of about 150° at magnification: a) 30000x, b) 1000x and c) 250x d) color mapping

[Downloaded from cehsat.iust.ac.ir on 2026-09-14]

[DOI: 10.22068/ijmse.3114]

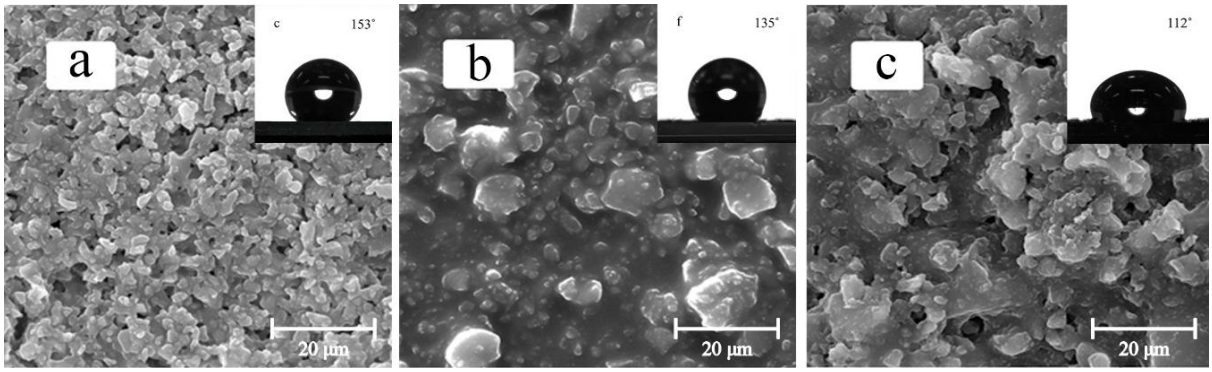

Fig. 5. SEM images of a) TSP3, b) TSP6 and c) TSP9 at 2000x magnification

Therefore, the water contact angle of the TSP6 sample has been reduced by about 20 degrees.

Figure 5 (c) compared to (a) indicated that doubling the amount of hydrophobic powder has significantly increased the agglomerate particle size. Consequently, the size of porosities has increased and the micro-nano structure of the surface has been destroyed. Similar to the TSP6 sample, the water contact angle in the TSP9 sample has also decreased, but the amount of reduction is about 40°.

In the TSP9 sample, the reason for the large reduction in the water contact angle is the irregular structure with micro particle size and porosity, which weakens the effect of reducing the surface energy of the -CH_3 functional groups [32, 33]. In the TSP6 sample, despite the integrated matrix without porosity, the water contact angle is larger than in the TSP9 sample, which shows the great effect of reducing surface energy on hydrophobic behavior. In the TSP3 sample, two mechanisms: 1-reduction of surface energy obtained from the functional groups -CH_3 and 2-micro-nano structure with porosities less than 10µm operate simultaneously and the coating shows superhydrophobic behavior with a water contact angle of 153° [13, 30].

FTIR analysis was performed to investigate the polymerization of polydimethylsiloxane and the modified surface of a hybrid of SiO_2–TiO_2 gels and the result is shown in Figure 6.

The 678 cm^{-1} peak indicates the presence of symmetric bonds O-Ti-O, which overlaps with the 693 cm^{-1} peak. The 693 cm^{-1} peak is consistent with tensile Si-C asymmetric bond. Further, the peaks at 805 cm^{-1} and 470 cm^{-1} could be ascribed to the Si-O-Si stretching vibrations, which are the characteristic peaks of SiO_2.

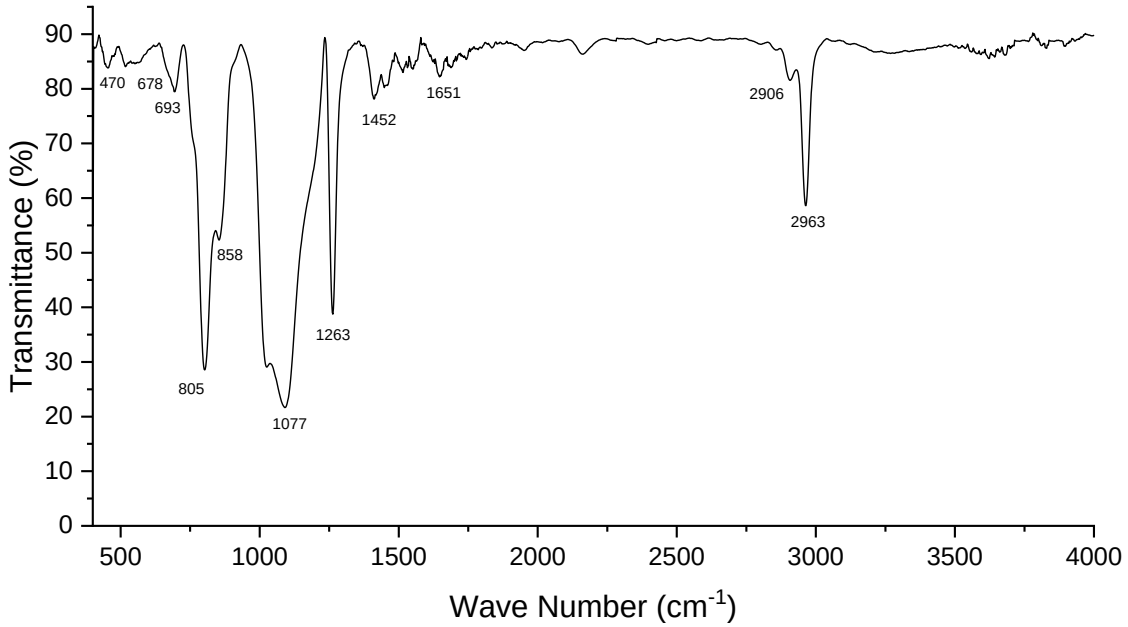

Fig. 6. FTIR peaks of a hybrid of SiO_2–TiO_2 gels

[Downloaded from cehsat.iust.ac.ir on 2026-09-14]

[DOI: 10.22068/ijmse.3114]

Also, 1077 cm^{-1} peaks show asymmetric tensile Si-O-Si groups [22]. Rosales et al. [21] also reported that the wide band of high intensity (1000–1100 cm^{-1}) corresponds to the characteristics signals of the Si-O-Si bonds in SiO_2. The 858 cm^{-1} peaks could be assigned to the copolymerization of PDMS with the Si-OH groups formed from the hydrolysis of TEOS [21]. Finally, 1261 cm^{-1}, 2905 cm^{-1} and 2962 cm^{-1} peaks correspond to flexural C-H bond symmetric, tensile C-H symmetric bond and tensile C-H asymmetric bond in $-CH_3$, respectively [18, 22]. The 1452 cm^{-1} corresponds to C-H absorption [26]. Also, the 1651 cm^{-1} peak is consistent with the C=C bond in the Vinyl group, respectively. From these interpretations, it can be concluded that the surface of nanoparticles was modified with $-CH_3$ groups and PDMS polymerization was performed [26]. Using non-flourinated chemicals like PDMS provided no concern for health or environment [34].

The photocatalytic properties of the TSP3 sample solution were evaluated under UV irradiation for the decomposition of the methylene blue molecule. The photocatalytic activity of the composition is expressed by a reduction in the concentration of methylene blue in an aqueous solution. The results of the degradation of methylene blue by SiO_2-TiO_2@PDMS under UV irradiation are shown in Fig.7. Because of its superior hydrophobicity, SiO_2-TiO_2@PDMS largely floated on the surface of methylene blue dilution. As a result, the methylene blue dilution could not be completely mixed with SiO_2-TiO_2@PDMS. Wang et al [18] also reported the same behavior for this composition. Within 20 minutes, the prepared blue solution began to discolor slowly. Under UV light irradiation for 120 minutes, the degradation rate of methylene blue was 55 percent, demonstrating that SiO_2-TiO_2@PDMS could degrade organic molecules to some extent. As suggested by Deng et al. [15], the reason for this is that titania gels have a large surface area and an imperfect anatase phase, which produces a large number of electron-hole pairs for the redox process when exposed to UV light. As a result, the SiO_2-TiO_2@PDMS coating was shown to be capable of photocatalytically decomposing organic pollutants. It was shown that the degradation rate of methyl orange with SiO_2-TiO_2@PDMS coating was 59% under UV light irradiation for 60 min [18]. Novotna et al. [35] declared that this composition can degrade MB up to 35% after 300 h. The difference in the degradation rate of organic dyes is due to the different amount of anatase in final coating.

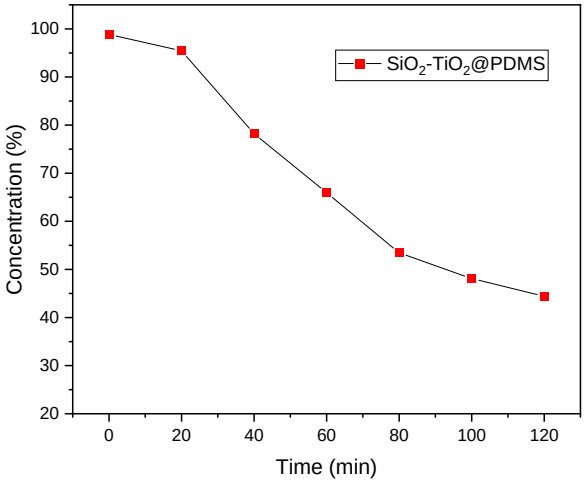

Fig. 7. Effect of photocatalytic degradation of TSP3 on methylene blue.

4. CONCLUSIONS

In this study, silica and titania nanoparticles were successfully produced by the sol-gel method. The surface of SiO_2-TiO_2 hybrid particles was modified using HMDS to form $-CH_3$ functional groups on their surface in order to increase the hydrophobicity and uniform distribution in the PDMS matrix. Consequently, the coating of SiO_2-TiO_2@PDMS on glass increased its contact angle from 30° to 152°. In addition, the best powder composition to produce a superhydrophobic coating in this method was 75% titanium and 25% silica, which provided the highest contact angle. The contact angle decreased with the increasing amount of silica. The sample's hydrophobicity was stable at high temperatures up to 400°C, before progressively switching to super hydrophilic at 450°C. Finally, it was found that increasing the amount of powder as well as increasing the concentration of PDMS in the coating solution reduced the contact angle compared to the initial composition and the optimal amount of composition was determined. Moreover, it was shown that the degradation rate of methylene blue was 55 percent under UV light irradiation, which indicates that SiO_2-TiO_2@PDMS could degrade organic molecules.

ACKNOWLEDGMENTS

[Downloaded from cehsat.iust.ac.ir on 2026-09-14]

[DOI: 10.22068/ijmse.3114]

This research did not receive any specific grant from funding agencies in the public, commercial, or not-for-profit sectors.

CONFLICT OF INTEREST STATEMENT

The authors declare that they have no known competing financial interests or personal relationships that could have appeared to influence the work reported in this paper.

REFERENCES

[1] Y. Bai, H. Zhang, Y. Shao, H. Zhang, J. Zhu, "Recent progresses of superhydrophobic coatings in different application fields: an overview", Coatings, 2021, 11, 116.

[2] M. Jin, Xing, Q. and Chen, Z., "A Review: Natural Superhydrophobic Surfaces and Applications", Journal of Biomaterials and Nanobiotechnology, 2020, 11, 110-149.

[3] D. Zhang, L. Wang, H. Qian, X. Li, "Superhydrophobic surfaces for corrosion protection: a review of recent progresses and future directions", Journal of Coatings Technology and Research, 2016, 13, 11-29.

[4] M. Ferrari, P. Piccardo, J. Vernet, F. Cirisano, "High transmittance superhydrophobic coatings with durable self-cleaning properties", Coatings, 2021, 11, 493.

[5] W. Li, Y. Zhan, S. Yu, "Applications of superhydrophobic coatings in anti-icing: Theory, mechanisms, impact factors, challenges and perspectives", Progress in Organic Coatings, 2021, 152, 106117.

[6] H. Chen, F. Wang, H. Fan, R. Hong, W. Li, "Construction of MOF-based superhydrophobic composite coating with excellent abrasion resistance and durability for self-cleaning, corrosion resistance, anti-icing, and loading-increasing research", Chemical Engineering Journal, 2021, 408, 127343.

[7] S. Rasouli, N. Rezaei, H. Hamedi, S. Zendehboudi, X. Duan, "Superhydrophobic and superoleophilic membranes for oil-water separation application: A comprehensive review", Materials & Design, 2021, 204, 109599.

[8] L. Zheng, H. Li, W. Huang, X. Lai, X. Zeng, "Light Stimuli-Responsive Superhydrophobic Films for Electric Switches and Water-Droplet Manipulation", ACS Applied Materials & Interfaces, 2021, 13, 36621-36631.

[9] P. Wu, Y. Deng, S. Fan, H. Ji, and X. Zhang, "A study on dissimilar friction stir welded between the Al–Li–Cu and the Al–Zn–Mg–Cu alloys," Materials, 2018, 11, 7, 1132.

[10] S.M. Alduwaib, M. M. Abd, I. mudher Hassan, "Facile Preparation and Characterization of SiO_2 Nanoparticles and Study of the Relation Between Contact Angle and Different Parameters", Iranian Journal of Materials Science and Engineering, 2022, 19, 1-9.

[11] J. Jeevahan, M. Chandrasekaran, G. Britto Joseph, R. Durairaj, G. Mageshwaran, "Superhydrophobic surfaces: a review on fundamentals, applications, and challenges", Journal of Coatings Technology and Research, 2018, 15, 231-250.

[12] S. Peng, W. Meng, J. Guo, B. Wang, Z. Wang, N. Xu, X. Li, J. Wang, J. Xu, "Photocatalytically Stable Superhydrophobic and Translucent Coatings Generated from PDMS-Grafted-SiO_2/TiO_2@PDMS with Multiple Applications", Langmuir, 2019, 35, 2760-2771.

[13] G. Barati Darband, M. Aliofkhazraei, S. Khorsand, S. Sokhanvar, A. Kaboli, "Science and Engineering of Superhydrophobic Surfaces: Review of Corrosion Resistance, Chemical and Mechanical Stability", Arabian Journal of Chemistry, 2020, 13, 1763-1802.

[14] C.R. Crick, J.C. Bear, A. Kafizas, I.P. Parkin, "Superhydrophobic photocatalytic surfaces through direct incorporation of titania nanoparticles into a polymer matrix by aerosol assisted chemical vapor deposition", Advanced Materials, 2012, 24, 3505-3508.

[15] Z.-Y. Deng, W. Wang, L.-H. Mao, C. -F. Wang, S. Chen, "Versatile superhydrophobic and photocatalytic films generated from TiO_2–SiO_2@ PDMS and their applications on fabrics", Journal of materials chemistry A, 2014, 2, 4178-4184.

[16] S.-J. Yang, X. Chen, B. Yu, H.-L. Cong, Q.-H. Peng, M.-M. Jiao, "Self-cleaning

[Downloaded from cehsat.iust.ac.ir on 2026-09-14]

[DOI: 10.22068/ijmse.3114]

superhydrophobic coatings based on PDMS and TiO_2/SiO_2 nanoparticles", Integrated Ferroelectrics, 2016, 169, 29-34.
[17] V. Crupi, B. Fazio, A. Gessini, Z. Kis, M.F. La Russa, D. Majolino, C. Masciovecchio, M. Ricca, B. Rossi, S.A. Ruffolo, "TiO_2–SiO_2–PDMS nanocomposite coating with self-cleaning effect for stone material: Finding the optimal amount of TiO_2", Construction and Building Materials, 2018, 166, 464-471.
[18] X. Wang, H. Ding, S. Sun, H. Zhang, R. Zhou, Y. Li, Y. Liang, J. Wang, "Preparation of a temperature-sensitive superhydrophobic self-cleaning SiO_2-TiO_2@ PDMS coating with photocatalytic activity", Surface and Coatings Technology, 2021, 408, 126853.
[19] P. Soroori, S. Baghshahi, A. Kazemi, N. Riahi Noori, S. Payrazm, A. Aliabadizadeh, "Room Temperature Cured Hydrophobic Nano-silica Coatings for Outdoor Insulators Installed on Power Lines without Shutting Down the Current", Iranian Journal of Materials Science and Engineering, 2022, 19, 1-12.
[20] M.G. RJ, V. Vidyadharan, S.M. Simon, A. Saritha, P. Biju, C. Joseph, N. Unnikrishnan, "Investigations on the blue luminescence enhancement of organically modified SiO_2-TiO_2-PDMS glass matrix", Nano-Structures & Nano-Objects, 2019, 20, 100377.
[21] A. Rosales, L. Ortiz-Frade, I.E. Medina-Ramirez, L.A. Godínez, K. Esquivel, "Self-cleaning of SiO_2-TiO_2 coating: Effect of sonochemical synthetic parameters on the morphological, mechanical, and photocatalytic properties of the films", Ultrasonics Sonochemistry, 2021, 73, 105483.
[22] P. Novotná, J. Matoušek, "Preparation and characterization of photocatalytical TiO_2–SiO2–PDMS layers on glass", Thin solid films, 2006, 502, 143-146.
[23] P. Seeharaj, P. Kongmun, P. Paiplod, S. Prakobmit, C. Sriwong, P. Kim-Lohsoontorn, N. Vittayakorn, "Ultrasonically-assisted surface modified TiO_2/rGO/CeO_2 heterojunction photocatalysts for conversion of CO_2 to methanol and ethanol", Ultrasonics sonochemistry, 2019, 58, 104657.
[24] V. Tajer Kajinebaf, M. Zarrin Khame-Forosh, H. Sarpoolaky, "Preparation and Characterization of Nanostructured Titania-coated Silica Microsphere Membranes with Simultaneous Photo-catalytic and Separation Applications for Water Treatment", Iranian Journal of Materials Science and Engineering, 2020, 17, 35-44.
[25] D. Arun Kumar, J. Merline Shyla, F.P. Xavier, "Synthesis and characterization of TiO_2/SiO_2 nano composites for solar cell applications", Applied Nanoscience, 2012, 2, 429-436.
[26] C. Kapridaki, P. Maravelaki-Kalaitzaki, "TiO_2–SiO_2–PDMS nano-composite hydrophobic coating with self-cleaning properties for marble protection", Progress in Organic Coatings, 2013, 76, 400-410.
[27] Y.-l. Yan, Y.-x. Cai, X.-c. Liu, G.-w. Ma, W. Lv, M.-x. Wang, "Hydrophobic Modification on the Surface of SiO_2 Nanoparticle: Wettability Control", Langmuir, 2020, 36, 14924-14932.
[28] Y. Qi, B. Xiang, W. Tan, J. Zhang, "Hydrophobic surface modification of TiO_2 nanoparticles for production of acrylonitrile-styrene-acrylate terpolymer/TiO_2 composited cool materials", Applied Surface Science, 2017, 419, 213-223.
[29] X. Liu, Y. Gu, T. Mi, X. Wang, X. Zhang, "Dip-coating approach to fabricate durable PDMS/STA/SiO_2 superhydrophobic polyester fabrics", Coatings, 2021, 11, 326.
[30] S. Parvate, P. Dixit, S. Chattopadhyay, "Superhydrophobic Surfaces: Insights from Theory and Experiment", The Journal of Physical Chemistry B, 2020, 124, 1323-1360.
[31] Z. He, M. Ma, X. Lan, F. Chen, K. Wang, H. Deng, Q. Zhang, Q. Fu, "Fabrication of a transparent superamphiphobic coating with improved stability", Soft Matter, 2011, 7, 6435-6443.
[32] Y. Cho, C.H. Park, "Objective quantification of surface roughness parameters affecting superhydrophobicity", RSC Advances, 2020, 10, 31251-31260.
[33] L. Li, J. Zhu, Z. Zeng, E. Liu, Q. Xue, "Effect of surface roughness on the angular

[Downloaded from cehsat.iust.ac.ir on 2026-09-14]

[DOI: 10.22068/ijmse.3114]

acceleration for a droplet on a super-hydrophobic surface", Friction, 2021, 9, 1012-1024.

[34] I. Torun, N. Celik, M. Ruzi, M.S. Onses, "Transferring the structure of paper for mechanically durable superhydrophobic surfaces", Surface and Coatings Technology, 2021, 405, 126543.

[35] P. Novotná, J. Zita, J. Krýsa, V. Kalousek, J. Rathouský, "Two-component transparent TiO_2/SiO_2 and TiO_2/PDMS films as efficient photocatalysts for environmental cleaning", Applied Catalysis B: Environmental, 2008, 79, 179-185.

[Downloaded from cehsat.iust.ac.ir on 2026-09-14]

[DOI: 10.22068/ijmse.3114]